LAWRENCE
LIVERMORE
NATIONAL
LABORATORY

LLNL-JRNL-804045

Modeling of Thermal Decomposition of TATB-Based Explosive for Safety Analysis

J. S. Moore, M. A. McClelland, P. C. Hsu, E. M. Kahl

January 31, 2020

Reaction Chemistry & Engineering

Disclaimer

Propellants, Explosives, Pyrotechnics

Full Paper

LLNL-JRNL-804045

DOI: 10.1002/prep.201((full DOI will be filled in by the editorial staff))

Modeling of Thermal Decomposition of TATB-Based Explosive for Safety Analysis

Jason S. Moore*[a], Matthew A. McClelland[a], Peter C. Hsu[a], and Evan M. Kahl[a]

Abstract: We investigate and model the cook-off behavior of LX-17 to understand the response of explosive systems in abnormal thermal environments. Decomposition has been explored via conventional ODTX (One-Dimensional Time-to-eXplosion), PODTX (ODTX with pressure-measurement), TGA (Thermo-Gravimetric Analysis), and DSC (Differential Scanning Calorimetry) experiments under isothermal and ramped temperature profiles. The data were used to fit reaction rate parameters for proposed schemes in an ALE3D computational model. This model includes chemical reactions, thermo- and hydro-dynamics, and material properties, including thermal expansion, compressibility, and strength. These parameterizations were carried out utilizing a Python evolutionary optimization method on LLNL's high-performance computing clusters. Additional experiments are being developed to further characterize and monitor decomposition intermediates to improve the model. Once experimentally validated, this model will be scalable to several applications involving LX-17. Furthermore, the optimization methodology developed herein should be applicable to other high explosive materials.

Keywords: TATB, Explosive Safety, Reaction Kinetics, ODTX

1 Introduction

Understanding the thermal response of energetic material is critical for response prediction and safe handling during and after exposure to high temperatures in accident scenarios. Formulations of the high explosive (HE) 1,3,5-triamino-2,4,6-trinitrobenzene (TATB), such as LX-17 (92.5% TATB, 7.5% Kel-F) and PBX-9502 (95% TATB, 5% Kel-F), are currently employed in industrial and military applications, due to their high thermal stability and low shock sensitivity. However, much is still not understood about the thermal decomposition pathways of TATB, including conflicting conclusions as to the effect of confinement[1] and whether the dominant decomposition mechanism includes gas-phase species.

Recent work by Hobbs and Kaneshige[1] included the effect of the initial water content, which is typically on the order of thousands of ppm, as determined by Small, Glascoe, and Overturf.[2] Including the water vapor-liquid equilibrium significantly improves the accuracy of pressure predictions during early decomposition, which is particularly important in low-confinement systems. Furthermore, several studies have shown that the decomposition of TATB yields a large quantity of water; experimental[3,4] and computational[5,6] studies indicate that the likely first step in decomposition is an intramolecular condensation reaction to form the benzo-monofurazan (MF), 5,7-dinitroisobenzofuran-4,6-diamine. TATB may also react to form the benzo-monofuroxan, 4,6-diamino-5,7-dinitrobenzo[c] [1,2,5] oxadiazole 1-oxide. However, little is known about what happens between these initial reactions and final thermal runaway. Experiments have shown that these intermediates can continue to dehydrate, and the furoxan species can be significantly less stable.[4,7] Additionally, some reported gas products, such as HCN, are highly hazardous and may require more precautions for first responders.[8]

Previous experiments related to hazards analysis have largely focused on thermal "cook-off" behavior in experiments such as the One-Dimensional Time to eXplosion (ODTX), which has recently been augmented with pressure measurements (PODTX).[9] Here, the "one-dimensional" refers to the use of a sphere of explosive material, allowing spatial considerations to largely be reduced to only a function of radius. This setup, shown in Figure 1, has been described elsewhere. In brief, a half-inch diameter sphere of HE is either exposed to a step-change in temperature by delivery to preheated anvils, which are rapidly closed, or subjected to controlled temperature ramps, sometimes with isothermal holds. This system can also be used to thermally damage samples to examine chemical and behavior changes without continuing to thermal runaway to assess changes in several safety metrics.[10] Critically, some partially decomposed samples have shown lower temperatures of thermal runaway with larger exotherms.

[a] *Lawrence Livermore National Laboratory Livermore, CA 94551*
E-mail: moore242@llnl.gov

Supporting information for this article is available on the WWW under http://www.pep.wiley-vch.de or from the author.

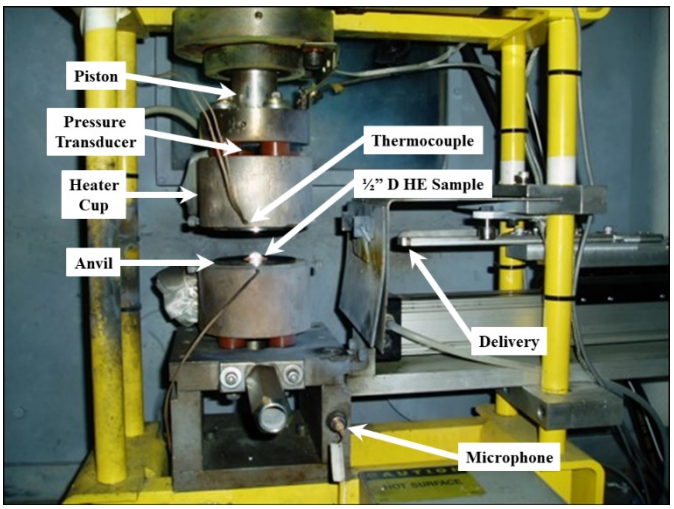

Figure 1. (P)ODTX experimental setup.[9]

As the focus of experiments thus far has largely been on end-point data, we recently proposed a more reduced form of the reaction network,[11] excluding the -furoxan species and later dehydration intermediates, which may not be along pathways necessary to reach final decomposition products. Our proposed reaction scheme is shown in Scheme 1, wherein TATB dehydrates intramolecularly, the mono-intermediate (MF) decompose inter-molecularly into gas and solid products, and the gas products further autocatalyze decomposition of TATB. The reaction stoichiometry was determined based upon assuming two dehydration steps and 21 wt% solid residue, as seen in thermo-gravimetric analysis (TGA). Our approach differs from previous modeling efforts in a few key respects. Firstly, our model uses only elementary reactions, excluding any elements lacking physical interpretation, such as Prout-Tompkins reactions[12,13] or fitting parameters.[1] Additionally, solid explosives differ from many traditional kinetic systems due to the large effect of spatially varying factors. Thus, experiments were simulated using ALE3D,[14] which includes chemical reactions, thermo- and hydro-dynamics, and material properties (see Supplemental Information), including thermal expansion, compressibility, and strength. Furthermore, the hydro-code enables the gas products to be modeled as a gas-phase concentration utilizing appropriate material properties, expansion, and compressibility dependent upon local conditions, rather than as a mixed phase species. In addition, we attempt to remedy a previous lack of kinetic model parameter error analysis in the TATB-based explosive literature.

$$H_2O_l \rightleftharpoons H_2O_g$$
$$TATB_s \xrightarrow{k_1} MF_s + H_2O_l$$
$$2MF_s \xrightarrow{k_2} 2Prod_g + 2H_2O_l + 9C_{amorph}$$
$$TATB_s + Prod_g \xrightarrow{k_3} 2Prod_g + 2H_2O_l + 4.5C_{amorph}$$

Scheme 1. TATB decomposition scheme.[11]

The end time in these experiments is determined when the pressure inside the anvils passes the holding pressure, typically 1500 or 2000 bar, depending on the exact experimental apparatus used. This event can occur by either explosion or by pressure burst – insufficient self-heating to produce thermal runaway. As shown in Figure 2, these experiments were modeled as a quarter circle of HE with axial and radial symmetry with a surrounding 1.5" radius shell of aluminum or stainless steel. For ODTX simulations, the aluminum shell was preheated to the appropriate temperature, allowing the adjacent surface of the HE to experience a rapid temperature change in the first fraction of a second of the calculation. For PODTX simulations, the temperature of the outer surface of a stainless-steel shell was ramped at the corresponding experimental rate. Ramp rates were tested from 0.1 to 10 °C/min. While at lower ramp rates, the experiment is predicted to be mostly isothermal, at higher ramp rates, significant thermal gradients are expected to exist, including between the inner and outer surface of the anvil, necessitating modeling of the full thickness.

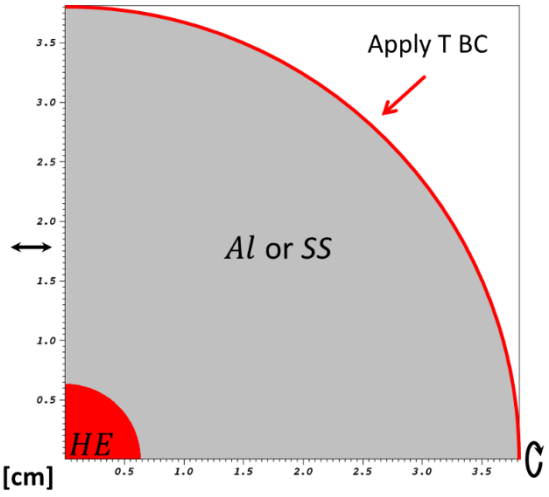

Figure 2. ALE3D (P)ODTX material diagram.

In addition to (P)ODTX[15] Time-To-eXplosion or pressure Burst (TTXB), (TGA), and differential scanning calorimetry (DSC) experiments were also simulated using ALE3D and compared to experimental results to fit kinetic parameters. Reaction rates for each of the three decomposition reactions, j, in Scheme 1,

$$k_j = k_{0,j} \exp\left[-\frac{E_{A,j}}{R}\left(\frac{1}{T}-\frac{1}{T_0}\right)\right] \quad (1)$$

where the activation energy, E_A, and the natural log of the orthogonalized pre-exponential factor, k_0, using ideal gas constant R and a reference temperature, T_0, of 588 K, were varied using the Python[16] SciPy[17] differential evolution algorithm.[18] The method was modified to update only after completing a generation rather than as each calculation finished to allow for parallelization and flexibility in use of computational resources.

The objective function

$$\sum_{i=1}^{N_{exp}} \left(ln\left({}^{t_{sim,i}}/_{t_{exp,i}} \right) \right)^2 \quad (1)$$

was minimized, where $t_{sim,i}$ and $t_{exp,i}$ are the simulated and experimental times, respectively, for the i^{th}

experiment. (P)ODTX calculations were stopped when the simulation time step dropped below 1 μs, indicating thermal runaway due to constraints on reaction extent change per integration step. This time was used as t_{sim}, unless the pressure at the boundary between the HE and anvils had already exceeded the holding pressure of 1500 or 2000 bar (see SI), in which case the time that pressure was reached was used. As TGA and DSC experiments were conducted on small samples of less than 10 mg in a pinhole pan, a different simulation was used to model these experiments, consisting of small zone of HE material sitting on an alumina block to simulate the temperature gradient in the alumina sample pan. A larger sample volume was simulated to approximate gas loss into the pan headspace. For TGA, the times at 0.5, 5, and 50% mass loss were compared. For DSC, the full-width half max of the exothermic peak was compared.

2 Results and Discussion

Simulations were run for a range of kinetic parameters to match experimental results for (P)ODTX, TGA, and DSC of wet-aminated LX-17-1 at several ranges of theoretical maximum density (TMD). Joint confidence intervals on k_0 and E_A for the first and third decomposition reactions indicated that these parameters were far more well determined than those for the decomposition of the MF intermediate, which only needed to react faster than a certain threshold rate. Thus, for the purposes of simulating end-point data, this intermediate reaction can be assumed to be rapid relative to the other steps and the first step can be modeled as going straight to the products, as is shown in Scheme 2 with parameters given in Table 1. The primary exotherm activation energy of 189.4 kJ/mol is within the range of previously determined values of 162 kJ/mol from Belmas *et al.*[19] to 251 kJ/mol from Bailey[20] and Rogers.[21] Additionally, while the product gas has been observed to contain several species,[3] the reaction rates in ALE3D utilize mass rather than mole concentrations, meaning specific product molecular weights and compositions did not have to be assumed.

$$H_2O_l \rightleftharpoons H_2O_g$$
$$TATB_s \xrightarrow{k_1} MF_s + H_2O_l$$
$$2MF_s \xrightarrow{Fast} 2Prod_g + 2H_2O_l + 9C_{amorph}$$
$$TATB_s + Prod_g \xrightarrow{k_3} 2Prod_g + 2H_2O_l + 4.5C_{amorph}$$

Scheme 2. Revised TATB decomposition scheme.

Table 1. Model parameters and 95% joint confidence intervals for Eq. 1 reaction rates shown in Scheme 2.

Parameter	Value	Units	Error
$ln\ k_{0,1}$	-11.06	s^{-1}	0.24
$E_{A,1}$	78.1	kJ/mol	12.2
$ln\ k_{0,3}$	8.71	$cm^3/g{\cdot}s$	0.22
$E_{A,3}$	189.4	kJ/mol	21.0

Resulting TTXB simulation and experimental results are shown in Figure 3. LX-17 end times used for fitting are compared in Figure 3a-b, including insets showing example temperature gradients within the HE at the end of the simulation, demonstrating the importance of radial effects of coupled chemistry and heat transfer. These insets show that at the higher temperatures, the outer layer of HE reacts rapidly before heat can conduct into the center. At lower temperatures, heat fully conducts into the HE, and thermal runaway occurs at the center when reaction heat production outpaces conduction. At lower temperatures still, thermal runaway may not occur, since the reaction may not reach this threshold. Figure 3c shows PBX-9502 and pressed coarse TATB results, which were not used for fitting.

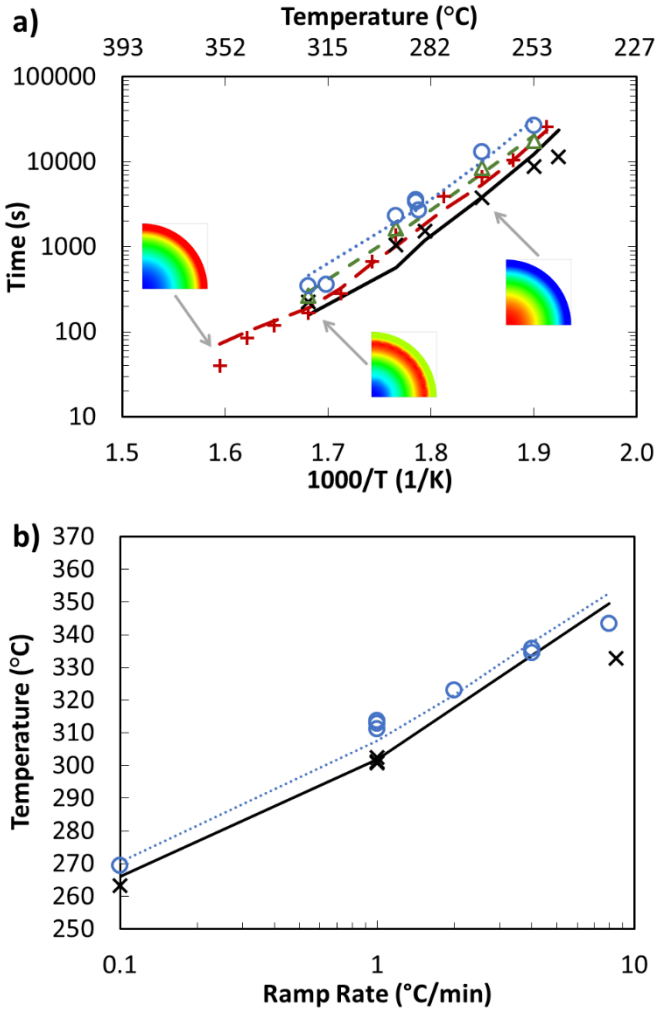

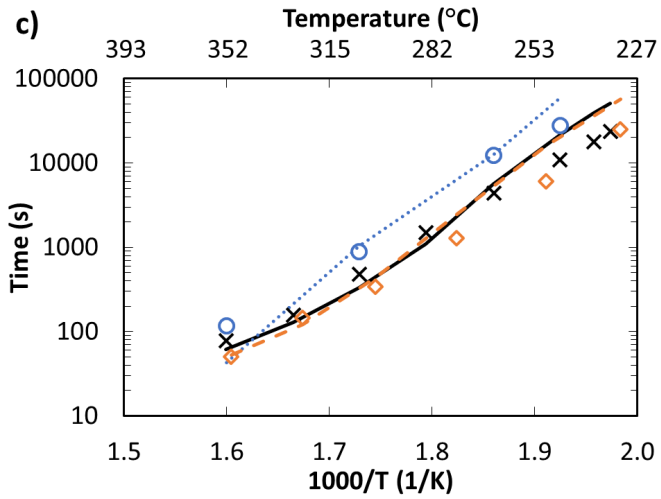

Figure 3. Experiment (symbols) and model (lines) explosion/burst time for a) LX-17 ODTX: 98-100% TMD (×; solid), 94-97% TMD (+; long dashed), 92-93% TMD (△; short dashed), and 85-89% TMD (○; dotted); b) LX-17 PODTX results: 98% TMD (×; solid) and 86% TMD (○; dotted); c) PBX-9502 ODTX results: 98-100% TMD (×; solid) and 85-89% TMD (○; dotted) and coarse TATB ODTX results: 98-100% TMD (◊; dashed).

The figure shows that both experimental and model results show a trend of increasing TTXB as TMD decreases. This feature is due to the use of the gas-phase product autocatalysis. Additionally, this gas-solid reaction would account for experimentally observed lower TTXB in ultrafine TATB as compared to coarse TATB of the same density (see Supplemental Information) due to increased specific surface area.[22]

One type of physics that is not fully implemented at present in the model is gas flow through the porous HE material and into any surrounding headspace due to concentration and pressure gradients. During heating, the HE can expand into available volume. The ODTX anvils were designed with 0.25-inch diameter inner cavities, which have only a few percent free volume at the edges due to the space between the sphere and the sealing gasket on the anvil surfaces. The PODTX anvils were designed with slightly larger 0.265-inch inner cavities, to allow for some HE expansion without plugging the pressure transducer channel. A thin metal sleeve is used in the lower half to provide better heat transfer between anvil and HE, but the upper half is left open, leaving approximately 10% additional free volume. Spheres of HE that have been heated in the PODTX setup show that they typically expand into this space (see Supplemental Information). Thus, for simulations, it is assumed that this extra air is uniformly mixed throughout the HE material. This assumption may not be accurate for short experiments performed at high temperatures or heating rates, which would explain the model discrepancies around 350 °C in Figure 3a-b.

Figure 4 shows experimental and modeled pressure of LX-17 at 1 °C/min heating rate for 98% and 86% TMD. While the TTXB is very similar for each plot, differences in pressure generation are visible. The effect of the water vapor-liquid equilibrium is prevalent from around its boiling point until diminishing in the last hour of experiment as additional product gases are formed. The lower density HE shows a monotonic increase, while the higher density appears noisier. It is likely that the lower density allows more gas permeation throughout the sample, while the higher density material keeps gas generation more local until pressure generation surpasses the solid strength, which decreases significantly with temperature, especially as the Kel-F binder melts. Thus, Figure 4b may be less representative of the true pressure experienced by the sample.

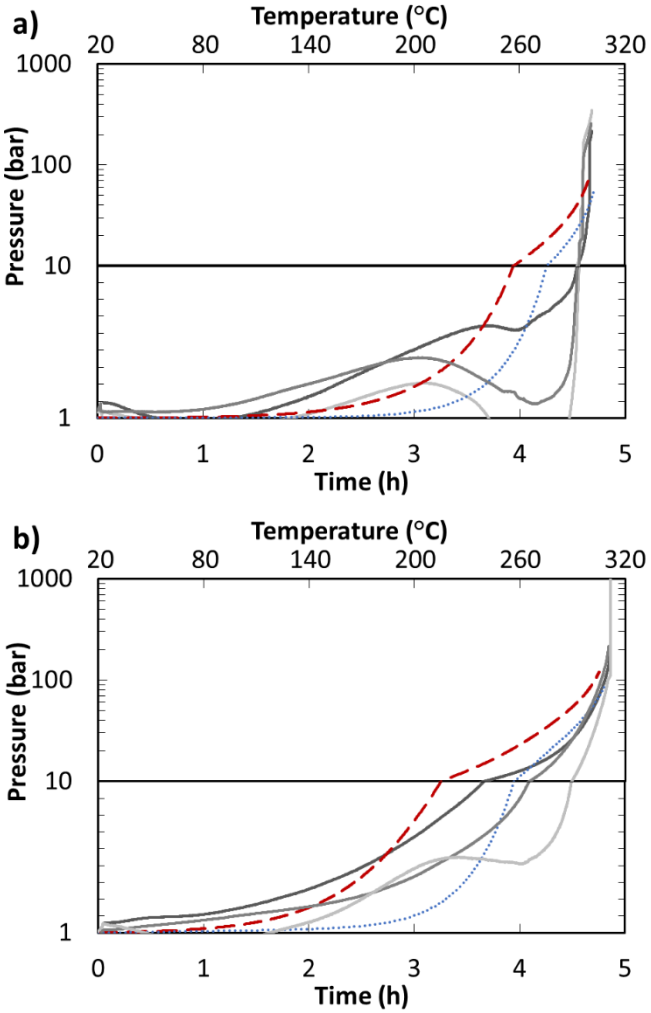

Figure 4. LX-17 PODTX pressure at 1 °C/min ramp. Three experimental repeats (gray solid lines), model with water (red dashed), and model without water (blue dotted) for a) 98% TMD; b) 86% TMD

Lastly, comparison of the 1 °C/min simultaneous TGA and DSC measurements and simulations are shown in Figure 5a-b, indicating the points used for data fitting. The early evaporation of the initial 0.15 wt% water is evident in the mass loss curve. The model also appears to capture the final rate of product catalysis and heat generation. However, in the middle temperature range, some mass loss in the experiment is not visible in the model. This discrepancy may be due to sublimation, which is not in

the model, as the (P)ODTX system is sealed and little sublimation is expected to occur; however, it may also be due to intermediate reactions that were not included in the reaction scheme. Both mechanisms would account for the endotherm in the DSC data, but determining which is occurring would require composition analysis of the solids or evolved gases, development of which is ongoing.[23,24] Thus, for purposes of comparison, the DSC data was shifted to remove the endotherm. The experimental heat-flow also shows a sharp thermal-runaway peak, which was not captured in the model. This indicates that there are likely multiple heating mechanisms, and that the most rapid exothermal behavior may require additional model detail.

With the high level of confinement used in the (P)ODTX systems, the early gas formation does not appear to have a significant impact on TTXB. However, in lower confinement systems, this may not be the case, as pressure burst is more likely to occur in the absence of thermal runaway and effects like the evaporation of water, which can easily contribute several tens of bar, become more important.

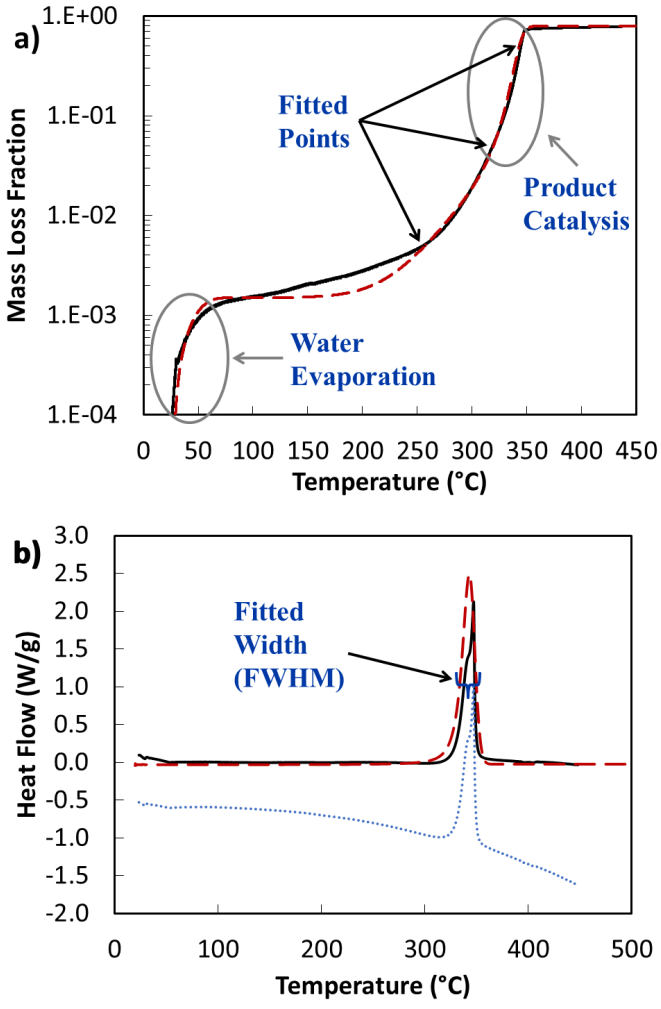

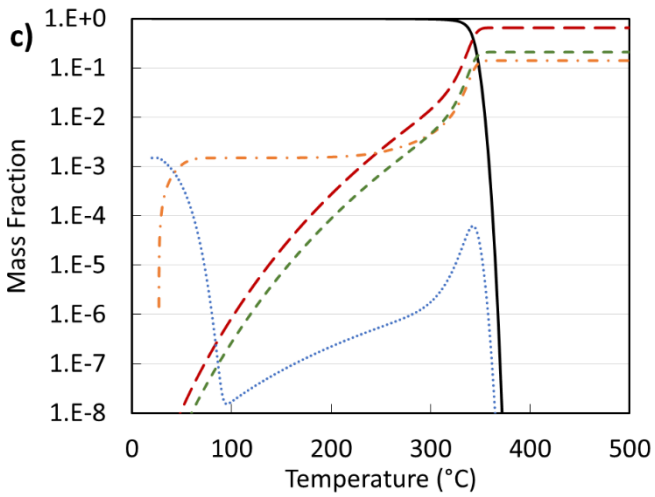

Figure 5. Results for TATB a) TGA experiment (black solid line) and model (red dashed line); b) DSC experiment (dotted blue line), experiment after endotherm subtraction (solid black line), and model (red dashed line); c) modeled concentrations for TATB (black solid line), product (red long-dashed line), amorphous carbon (green short-dashed line), water (blue dotted line), and steam (orange dash-dot line).

3 Conclusion and Future Outlook

LX-17 cook-off was modeled with ALE3D and compared to several experiments. This model captures a significant portion of the behavior of the experiments with only four fitted parameters. Time-to-explosion was well predicted under isothermal and ramped heating conditions. However, intermediate and individual product species were not modeled, and understanding their concentration evolution would be critical to predicting sensitization behavior and handling concerns.

Experiments are currently under development to better answer questions related to the reaction network through intermediate species. This ongoing work aims to measure chemical composition of reaction products in both solid and gas phases during experiments, as well as analysis of solid residue in aged and spent materials. Where possible, online analysis via infrared spectroscopy should be used to determine key intermediates and to track the time evolution of their concentrations isothermally at multiple temperatures and at different ramp rates. Ideally, these experiments should look both directly at the headspace in the pressure vessel and at the solid, possibly through an integrated attenuated total reflectance lens.

Offline analysis with mass spectrometry is less ideal, as time-dependent data cannot be generated easily with a single experiment. However, the additional ability to determine chemical species makes this technique highly valuable, especially when used to relate back to the IR experiments to pinpoint the actual species that contain the moieties present. These results should significantly inform model development and allow intermediate reactions to be better defined and parameterized with confidence, which has largely

not been possible relying solely on time-to-explosion endpoint data.

Acknowledgements

This work was performed under the auspices of the U.S. DOE by LLNL under contract DE-AC52-07NA27344. LLNS, LLC. The authors wish to thank Ben Yancey and Jennifer Montgomery for DSC and TGA data, Steve Strout for (P)ODTX runs, and John Reynolds for sensitization analysis.

Disclaimer

References

[1] M. L. Hobbs and M. J. Kaneshige, "Ignition Experiments and Models of a Plastic Bonded Explosive (PBX 9502)," *The Journal of Chemical Physics,* vol. 140, **2014**.

[2] W. Small IV, E. A. Glascoe and G. E. Overturf, "Measurement of Moisture Outgassing of the Plastic-Bonded TATB Explosive LX-17," *Thermochimica Acta,* vol. 545, pp. 90-95, **2012**.

[3] T. A. Land, W. J. Siekhaus and M. F. Foltz, "Condensed-Phase Thermal Decomposition of TATB Investigated by Atomic Force (AFM) and Simultaneous Thermogravimetric Modulated Beam Mass Spectrometry (STMBMS)," in *International Detonation Symposium*, Boston, **1993**.

[4] J. Sharma, J. W. Forbes, C. S. Coffey and T. P. Liddiard, "The Physical and Chemical Nature of Sensitization Centers Left from Hot Spots Cause in Triaminotrinitrobenzene by Shock or Impact," *Journal of Physical Chemistry,* vol. 91, pp. 5139-5144, **1987**.

[5] C. J. Wu and L. E. Fried, "Ring Closure Mediated by Intramolecular Hydrogen Transfer in the Decomposition of a Push-Pull Nitroaromatic :TATB," *Journal of Physical Chemistry A,* vol. 104, pp. 6447-6452, **2000**.

[6] Q. Wu, H. Chen, G. Xiong, W. Zhu and H. Xiao, "Decomposition of a 1,3,5-Triamino-2,4,6-trinitrobenzene Crystal at Decomposition Temperature Coupled with Different Pressures: An ab Initio Molecular Dynamics Study," *Journal of Physical Chemistry C,* vol. 119, pp. 16500-16506, **2015**.

[7] R. R. McGuire, "Properties of Benzotrifuroxan," Lawrence Livermore National Lab, Livermore, CA, **1978**.

[8] E. Catalano and C. E. Rolon, "A Study of the Thermal Decomposition of Confined Triaminotrinitrobenzene.," *Thermochimica Acta,* vol. 61, pp. 37-51, **1983**.

[9] P. C. Hsu, M. Howard and J. L. Maienschein, "The ODTX System for Thermal Ignition and Thermal Safety Study of Energetic Materials," in *International Detonation Symposium*, Coeur D'Alene, ID, **2010**.

[10] E. M. Kahl, P. C. Hsu, K. R. Coffee, B. J. Yancey, A. J. Nelson, H. E. Mason, G. F. Ellsworth, T. E. Healy, J. C. Crowhurst, T. W. Myers and J. G. Reynolds, "Safety Assessment of Thermally Damaged Energetic Materials," in *International Detonation Symposium*, Cambridge, MD, **2018**.

[11] J. S. Moore, M. A. McClelland, P. C. Hsu, G. F. Ellsworth, E. M. Kahl and H. K. Springer, "Thermal Safety Modeling of TATB-based Explosive," in *International Detonation Symposium*, Cambridge, MD, **2018**.

[12] E. G. Prout and F. C. Tompkins, "The Thermal Decomposition of Potassium Permanganate," *Transactions of the Faraday Society,* vol. 40, pp. 488-498, **1944**.

[13] J. Koerner, J. Maienschein, A. Burnham and A. Wemhoff, "ODTX Measurements and Simulations on Ultra Fine TATB and PBX-9502," in *North American Thermal Analysis Society*, East Lansing, MI, **2007**.

[14] C. Noble, A. Anderson, N. Barton, J. Bramwell, A. Capps, M. Chang, J. Chou, D. Dawson, E. Diana, T. Dunn, D. Faux, A. Fisher, P. Greene, I. Heinz, Y. Kanarska, S. Khairallah, B. Liu, J. Margraf, A.

Nichols III, R. Nourgaliev, M. Puso, J. Reus, P. Robinson, A. Shestakov, J. Solberg, D. Taller, P. Tsuji, C. White and J. White, "ALE3D: An Arbitrary Lagrangian-Eulerian Multi-Physics Code," LLNL-TR-732040, Lawrence Livermore National Laboratory, **2017**.

[15] When ODTX and PODTX are discussed together, “(P)ODTX” is used.

[16] Python Software Foundation, "Python 2.7," https://docs.python.org/2.7/, **2018**.

[17] E. Jones, T. Oliphant and P. Peterson, "SciPy: Open source scientific tools for Python," **2001**. [Online]. Available: http://www.scipy.org/. [Accessed 2017].

[18] R. Storn and K. Price, "Differential Evolution - a Simple and Efficient Heuristic for Global Optimization over Continuous Spaces," *Journal of Global Optimization,* vol. 11, pp. 341-359, **1997**.

[19] R. Belmas, A. Bry, C. David, L. Gautier, A. Keromnes, D. Poullain and G. Theveno, "Preheating Sensitization of a TATB Composition Part One: Chemical Evolution," *Propellants, Explosives, and Pyrotechnics,* vol. 29, no. 5, pp. 282-286, **2004**.

[20] P. B. Bailey, "On the Problem of Thermal Instability of Explosive Materials," *Combustion and Flame,* vol. 23, pp. 329-336, **1974**.

[21] R. N. Rogers, "Thermochemistry of Explosives," *Thermochimica Acta,* vol. 11, pp. 131-139, **1975**.

[22] C. M. Tarver and J. G. Koerner, "Effects of Endothermic Binders on Times to Explosion of HMX- and TATB-Based Plastic Bonded Explosives," *Journal of Energetic Materials,* vol. 26, pp. 1-28, **2008**.

[23] E. M. Kahl, N. K. Muetterties, A. J. Nelson, H. E. Mason, J. V. Crowhurst, K. R. Coffee, J. S. Moore and J. G. Reynolds, "Characterization of Solid Residue Formation in LX-17 Exposed to Abnormal Thermal Environments," in *American Physical Society: Shock Compression of Condensed Matter*, Portland, OR, **2019**.

[24] G. L. Klunder, N. K. Muetterties, E. M. Kahl, P. E. Spackman and P. C. Hsu, "Compositional One-Dimensional Time to Explosion," in *International Detonation Symposium*, Cambridge, MD, 2018.

[25] C. M. Tarver, S. K. Chidester and A. L. Nichols, "Critical Conditions of Impact- and Shock-Induced Hot Spots in Solid Explosives," *Journal of Physical Chemistry,* vol. 100, pp. 5794-5799, **1996**.

Received: ((will be filled in by the editorial staff))
Revised: ((will be filled in by the editorial staff